https://doi.org/10.5194/nhess-2021-16
Preprint. Discussion started: 19 February 2021

Natural Hazards and Earth System Sciences
Discussions

Evolution of the Tazones Lighthouse slope (Cantabrian coast, N Spain). Multidisciplinary monitoring between 2018 and 2020

María José Domínguez-Cuesta[1], Pelayo González-Pumariega[2], Pablo Valenzuela[3], Carlos López-Fernández[1], Manuel Mora[4], Mónica Meléndez[5], Fernando Herrera[1], Miguel Ángel Marigil[6], Luis Pando[1], José Cuervas-Mons[1], Montserrat Jiménez-Sánchez[1]

[1]Department of Geology, University of Oviedo, Oviedo, Spain, Oviedo, 33005, Spain
[2]Department of Mining Exploitation and Prospecting, University of Oviedo, Mieres, 33600, Spain
[3]Tecnologías y Servicios Agrarios, Tragsatec S.A., León, 24008, Spain
[4]Delegación Territorial en Castilla y León, Agencia Estatal de Meteorología, Valladolid, 47014, Spain
[5]Oficina de Oviedo, Instituto Geológico y Minero de España, Oviedo, 33005, Spain
[6]Delegación de Asturias, Instituto Geográfico Nacional, Oviedo, 33007, Spain

Correspondence to: María José Domínguez-Cuesta (dominguezmaria@uniovi.es)

Abstract. The Tazones Lighthouse slope shows different active mass movements affecting an area of 70.000 m^2 of the Cantabrian Coast (N Spain), characterized by almost vertical rocky cliffs developed on Jurassic rocks: alternating marl, sandstone and limestone with three main stratigraphic and structural discontinuity families. Between June 2018 and May 2020, 22 monthly monitoring campaigns have been carried out to measure the displacement of 38 control points, located between 95-110 masl. The total station monitoring has been complemented by ortophoto analysis and detailed digital terrain models (DTM) from two drone flights. Since the beginning of the 3D monitoring, about the 50% of the markers moved more than 1 m, one of them exceeding 15 m. Detailed DTM has shown that the increased activity is controlled by the discontinuities. There is an extraordinary correlation between displacement acceleration and precipitation and soil moisture: the largest displacements have occurred after 2 periods of intense rain (January and October-November 2019, with a maximum 24-hour precipitation of 64.5 mm and 82.1 mm, respectively, and soil moisture values higher than 90%). This represents an exceptional opportunity to analyse in real time the Jurassic cliffs retreat of the Cantabrian Coast, a question that remained not quantified.

1 Introduction

The coast is a natural system very sensitive to environmental and climatic changes, responding quickly to them. In the current global warming scenario, climate projections indicate that sea level rise will continue and, most likely, increase the frequency and intensity of extreme rainfall events. These factors, together with changes in atmospheric circulation, regime of winds and associated waves, will affect coastal geomorphological activity (Nicholls, 2011). Therefore, an increase in slope instabilities, considered one of the most important processes of coastal retreat, could be expected on the cliffs.

Usually the interest in the coast retreat has mainly focused on the sandy coasts, that is, areas of beaches and estuaries, especially attractive for human occupation and tourism (McGranahan, 2007; Athanasiou et al., 2020). However, the rocky coasts, that

https://doi.org/10.5194/nhess-2021-16
Preprint. Discussion started: 19 February 2021


Natural Hazards and Earth System Sciences Discussions

represent, considering different authors from 52% (Young and Carilli, 2018) until 75-80% of coasts worldwide (Emery and Kuhn, 1982; Trenhaile, 1987; Sunamura, 1992), are increasingly the object of research to find out how they will evolve in the short-medium term (Trenhaile, 2014). More than one third (37%) of the Atlantic continental European coastline is a rocky coast along approximately 3,666 km (Gómez-Pujol et al., 2014). Active cliffs are considered to be a source of sediment that contributes to maintaining adjacent coastal environments and the resilience of the system at a wider scale (EUROSION, 2004). Natural hazard situations are common in these areas, due to both limitations in the space available to accommodate natural retreat and human occupation.

The Cantabrian coast, located in the North of the Iberian Peninsula, is an eminently rocky and abrupt E-W trending line along 800 km. Almost 200 of them, mainly rocky cliffs, belong to the Asturias region, where slope instabilities are frequent (Valenzuela et al., 2017; Domínguez-Cuesta et al., 2018a; 2018b). There are numerous studies focused on the loss of sand or the general evolution of the Cantabrian coast beaches (Flor and Flor-Blanco, 2005; Flor et al., 2015; Flor-Blanco et al., 2015; Blasco et al., 2018), but few are focused on the characterization of the rocky cliffs retreat (Domínguez-Cuesta et al., 2020a; 2020b). However, some previous works have obtained average retreat rates of 0.57 m year^{-1} for the period 2006-2017, reaching rates up to 1.22 and 2.19 m year^{-1} near the town of Luanco, in the surroundings of Peñas Cape (Domínguez-Cuesta et al., 2020a). Although these retreat values corresponds to specific areas, they are values similar to those obtained in Fisterra, Northern Spanish Atlantic coast (range 0.03 – 2.78 m year^{-1}, Pérez-Alberti et al., 2013), much higher than the established in the central coast of Portugal (range 0.013 – 0.130 m year^{-1}, Epifânio et al., 2013) or the Atlantic rocky coast (Gómez-Pujol et al., 2014 and references therein) and they agree with those reported in Holderness, considered the most active coast in Europe, with values of 2 m year^{-1} (Bird, 2008; Castedo et al., 2015; Hobbs et al., 2020).

As occurs throughout the world, in the region of Asturias, the coast is the area preferably occupied by humans since prehistoric times (Turrero et al., 2013). Thus, the coastal retreat generates social and economic vulnerability due to the population density, industrial activity, cultural heritage and exposed infrastructures of the coastal municipalities. The geomorphological evolution of the rocky cliffs is mainly due to mass movements linked to gravity and marine dynamics processes that cause its retreat. Taking into account the above, the research project in which this work is framed was launched to qualitatively and quantitatively characterize the retreat of the Asturian coast, using the cliff instabilities as indicator (Domínguez-Cuesta et al., 2019). It is necessary to know in depth how natural processes occur, to incorporate geological risk into land management and urban planning, as has already been shown in other parts of Spain (Mateos et al., 2017) and the world (Boualla et al., 2019).

The eastern-central segment of the Asturian coast (27% of the Asturian coastline) is composed of Jurassic-Cretaceous bedrock characterized by a subhorizontal or slightly inclined bedding and an alternation of siliceous-calcareous rocks (Valenzuela et al., 1986; García-Ramos and Aramburu, 2010; Piñuela, 2015). This area is internationally known as The Dinosaur Coast because of its remarkable paleontological heritage characterized by the abundance of dinosaur and other Jurassic reptile footprints and bones (Piñuela et al., 2016; Rauhut et al., 2018). It has been officially declared as the Asturian Tracksites Natural Monument-Yacimientos de Icnitas de Asturias (45/2001 Decree, of April 19th, BOPA 106 of May 9th, 2001). The scarps of old mass movements are visible along the entire Jurassic coast. In fact, the activity by gravity processes in the Jurassic cliffs

https://doi.org/10.5194/nhess-2021-16
Preprint. Discussion started: 19 February 2021


Natural Hazards and Earth System Sciences Discussions

of this area allows to obtain new samples of paleontological interest each year (López-Toyos et al., in press). However, until now the movement mechanisms and the speed at which this type of mass movement processes takes place have not been characterized in detail.

The Tazones Lighthouse slope shows active mass movements affecting a stretch of the coast of approximately 600 m characterized by the presence of almost vertical rocky cliffs developed on Jurassic rocks (Fig. 1). The different instabilities of the Tazones Lighthouse slope constitutes an outstanding opportunity to understand the complex evolution mechanisms of the rocky cliffs in coastal areas of temperate climate with bedrocks composed by lithological alternation. Thus, the aims of this work are to: i) Characterize the type, spatial distribution and recent evolution of the instabilities; ii) Quantify its spatial and temporal displacement during the period June 2018 – May 2020; and iii) Understand the role of geological and climatic factors.

1.1 Setting

The study area of the Tazones Lighthouse slope (43°32'54"N, 5°23'57"W) includes a sector of 161,103 m^2 characterized by the presence of a marine terrace (rasa) located at 115 m.a.s.l. limited by almost vertical rocky cliffs developed on Jurassic rocks (Fig. 1).

The bedrock of the Tazones lighthouse area is composed of marl alternating with gray and ocher or yellow-brown sandstone and rare intercalated marly limestone layers. These rocks, belonging to the Lastres Formation (Upper Jurassic), represent an ancient fluvial-dominated deltaic system with NE orientation (García-Ramos and Aramburu, 2010). The quartzarenite sandstone appear in 1-10 m bodies, alternating with 5-15 m levels of marls and shelly mudrocks in layers of centimetric to decimetric thickness. The sandstone beds of the Lastres Formation present both quartz and carbonate (ferrous calcite) cement; this latter is what gives it the ocher or yellow-brown tones when it is weathered in the recent outcrops: the more yellow-ocher the layer, the more ferrous calcite content and weathering intensity. Carbonate cement comes from transgressive muddy and sandy shell beds located above the sandstone bodies and infill partially the initial pores of the sandstone. Thus, the muddy shell beds behave like marls. Later, in a more advanced diagenetic stage, the remainder pores are filled by quartz cement (García-Ramos, 2013). The Quaternary coverage present in the area corresponds to patches of colluvium deposits whose depth does not exceed 2 m.

Jet black mining activities were common over the Mesozoic Asturian coast since the Middle Age (Monte Carreño, 2004). This fossil wood was extracted by means of the excavation of small galleries through the softest lithologies. Several jet mining have been reported in the surroundings of the Tazones Lighthouse area (Bahamonde et al., 1986), including an old abandoned mining exploitation known as Monte San Miguel within the study area (López, 2012). Indeed, preexistent subsidence points in the meadows area surrounding the lighthouse have been traditionally interpreted as collapses of jet mining galleries (Monte Carreño, 2004) and are described in this way on the municipal land-use planning.

The Asturian region show a characteristic Oceanic climate. According to the Köppen-Geiger classification (Peel et al., 2007) the climatic domain present in the study area is Temperate climate Cfb, characterized by a temperate summer and without dry season (García Couto, 2011). Precipitation and temperature show annual average values of 1000 mm yr^{-1} and 13°C,

https://doi.org/10.5194/nhess-2021-16
Preprint. Discussion started: 19 February 2021


Natural Hazards and Earth System Sciences Discussions

respectively. This facilitates the proliferation of vegetation that covers the entire study area, with a predominance of meadows and eucalyptus plantations, in addition to scrub areas.

The area is being monitored since 2018, when irreversible structural damages appeared in a restaurant building (Fig. 2a) located in the surroundings of the lighthouse because of the fast evolution of the landslide (Domínguez-Cuesta et al., 2019, 2020b; Valenzuela et al., 2019). The towns of Villar and Tazones area located in the vicinity of the study area, although outside of it. Within the studied area there were only three constructions: a vacation house, the Tazones Lighthouse and the mentioned restaurant, demolished as a result of the gravity process activity. The area is highly frequented by tourists who come to see the lighthouse and to walk a section of the Asturian coastal path that runs through the surroundings, known as the Jet Route trail-Ruta del Azabache. At the bottom of the cliff, it is also frequent the presence of fishermen or visitors who come to recognize dinosaur tracks or to take a walk.

2 Methodology

Methodology includes a multimethod approach with diverse tasks such as: (i) field work to carry out geomechanical characterization of the cliffs' bedrock, (ii) topographic markers installation and monthly topographical auscultation operations, (iii) annually photogrammetric surveys by Remotely Piloted Aircraft (RPA), (iv) photointerpretation, (v) installation of a rain gauge and precipitation and soil moisture content data compilation, and (vi) integration and analysis of all data by Geographical Information System, GIS (ArcGIS v10.3).

The geomechanical characterization of the rock has been carried out by surveying four geomechanical stations at the foot of the cliff (Fig. 1a), which is the only accessible area where the bedrock outcrops. Moreover, an overall inspection of the cliff has been performed from a boat from the sea.

Slope displacement has been topographically monitored through 34 feno-type markers and 4 additional control points, distributed in an area of approximately 12,000 m^2 (Fig. 1b). Before its installation, a preliminary field reconnaissance of the area was carried out to try to ensure that their positions allowed measuring the displacement in the direction of the cracks opening. In June 2018, 24 topographic markers were installed; 10 more were added in December of that year and 2 additional ones were installed in February 2019, after the appearance of new cracks. All of them are located in the range 95-110 meters above sea level. From the first date outlined until May 2020, 22 topographic control campaigns have been carried out (the installation one, plus 21 follow-up campaigns), attempting that their periodicity was monthly, although the time intervals from one to the other range from 16 to 75 days (Table 1).

The instrument used to observe the control points was a Leica TC-407 total station (precision of the angular measurement = 7"; precision of the distance measurement = 2 mm ± 2 ppm). Given the configuration of the terrain and the observation methodology used, displacements less than 2 cm are not considered significant. In order to facilitate the handling and interpretation of the results of the topographic measurements, an arbitrary coordinate system was adopted, so that the abscissa axis sensibly coincides with the direction in which the greatest movements of the ground occur.

https://doi.org/10.5194/nhess-2021-16
Preprint. Discussion started: 19 February 2021


Natural Hazards and Earth System Sciences Discussions

Due to the rapid evolution of the landslide, two of the control points were lost, between January and February 2019 (FA1) and between November and December 2019 (ARB); a bulldozer destroyed a marker located on a concrete water tank (CA8) and partially affected another one (FA9). Thus, some topographic markers appear without data, either because (i) they began to be measured from the second installation in December 2018, (ii) some of them have been lost, or (iii) other different problems occurred during the monthly measurement of that point. All the displacement data measured in each campaign were integrated into a GIS and represented both in maps and Excel charts.

Two photogrammetric surveys have been done by Remotely Piloted Aircraft (RPA) on November, 17 2018 and November, 29 2019. The aircraft used is CÁRABO S3 (ICOM3D), a robust and compact quadcopter with the following sensor specifications: Sony A5100 with Exmor® CMOS Sensor type APS-C (23.5 x 15.6 mm), with 16mm or 20mm fixed lens. As a result, textured 3D Cloud with an average point density of 25 pts m^{-2}, Digital Surface Models (DSM) from the obtained 3D clouds and high resolution Orthophotos with a 3 cm GSD have been obtained for each year. All these has been generated from the partial images taken by the Cárabo S3: 169 in 2018 and 162 in 2019. The comparison between both DSM was carried out using Cloud Compare v2.10.2. It allowed to show up the changes occurred on the slope of the Tazones Lighthouse surroundings and compare it to its 2018 appearance, expressing the changes in absolute distances (m).

Photointerpretation was made from aerial photographs, and sequential satellital images (Google Earth) from different years since 2001 to 2016, and from the images obtained in 2018 and 2020 by RPA.

The precipitation data of 4 rain gauges of the Agencia Estatal de Meteorología-Spanish Meteorological Agency (AEMET) were compiled for the period January 2018 – May 2020: Colunga (12.5 km far), Gijón-Campus (19.3 km), Luces-Aspo (10.0 km) and Candanal de Villaviciosa (16.6 km). Furthermore, in the context of this research, a new AEMET manual rain gauge was installed in Oles village (2.3 km far from Tazones Lighthouse) and managed by volunteers, but it only could provide discontinuous data between November 2018 and January 2020. The recorded data were compared with those of the mentioned four meteorological gauges in order to select the most representative. It was found that the Luces-Aspo station had a complete series of data with good correspondence with those recorded at the Oles station. Therefore, the precipitation data registered in Luces-Aspo rain gauge (43°03'10"N, 5°17'33"W), 10 km far from study area, 1 km far from the coast and with similar monthly-accumulated precipitation values, have been used in this work. The accumulated precipitation between each measurement campaign dates (approximately but not exactly month elapsed) was calculated and plotted in temporal graphs, in order to better establish the markers movement and its correlation with precipitation.

The soil moisture content has been characterized through the analysis of the Available Water Capacity (AWC), a hydrological index that has previously proved to be suitable for the study of the landslide-triggering processes (Valenzuela et al. 2018). AWC has been calculated as a percentage of the maximum pore water storing capacity of the soil volume limited by the depth of the vegetation roots. The analyzed daily data have been extracted for the same study period from Daily Water Balance Models developed by AEMET for the Spanish territory (Botey and Moreno, 2012).

All the information has been managed by GIS allowing to integrate all the data and to establish the spatio-temporal evolution of the Tazones Lighthouse slope.

https://doi.org/10.5194/nhess-2021-16
Preprint. Discussion started: 19 February 2021


Natural Hazards and Earth System Sciences Discussions

3 Results and discussion

The results are presented and discussed below in two sections: (1) Description of the Tazones Lighthouse slope instability: spatial distribution, recent evolution and geological factors, and (2) analysis of quantitative measurements of slope displacement for the period June 2018 – May 2020 and the role of precipitation and soil moisture content.

3. 1 Slope instability evidence and geological factors

The portion of the slope in which evidence of activity by mass movements can be recognized occupies an area of 70,000 m^2. It presents a ranging altitude between 110 and 0 meters. The slopes are gentle or flat in the upper zone (Fig. 1b), corresponding to the rasa area (15.4% of the surface, with slope under 10°), where meadows predominate. The slope increases in the middle part, where tree vegetation of eucalyptus plantations predominates, and it is especially high on the cliff with almost no vegetation (75% of the surface presents slopes between 10 and 50° and 9.6% between 50 and 82°).

In the upper part of the slope, main evidence of instability corresponds to different cracks (Fig. 2). The first evidences were recognized when the investigators came to the area, in February 2018, during the eviction of the restaurant due to the opening of the cracks that irreversibly affected the structure of the building (Fig. 2ba). It could be noticed that some of the cracks were old and other showed signs of recent activity, progressing until now. Both, the vacation house and the lighthouse are outside of the cracked area.

The data taken in the four geomechanical stations (Fig. 1a, Fig. 2e) have allowed geologically and geotechnically characterizing the bedrock by defining three main families of discontinuities (S0: 360/15-17; J1: 262/85; J2: 166/75), whose intersection favors the individualization of bedrock blocks. This is very evident in the central part of the monitored area, where different blocks can be recognized. Its size ranges between 3x3x6 m and 9x9x6 m, conditioned by the mentioned thickness of the Lastres Fm. layers and the spacing between the joints (Fig. 2c, d).

Figure 3 shows the temporal evolution of the cracks in the area. Some of them were already partially visible in the 2001 images (Fig. 3a). Even some small stretches can be intuited in old aerial photographs of up to 1984 (López-Toyos et al., in press). However, although they are spatially coincident with the area of current activity, the description of jet mining galleries collapses in the area by some authors (Monte Carreño, 2004) hampers to unequivocally know the origin of these signs.

The cracks were clearly visible in 2016 (Fig. 3b), but showed a fast growing from 2018 (Fig. 3c) to 2019 (Fig. 3d), reaching a total cumulative length of about 1,000 m, a maximum width of 8 m and 10 m maximum depth. As shown by Fig. 3c, there is a close relationship between the cracks trending and the position of J1 and J2 joints families. The cracks are still presently growing, because of the activity of the slope.

Three main areas can be distinguished according to the distribution of slopes indicated above (Fig. 1b): (i) upper area of very low slope and predominantly without movement (blue in Fig. 4a), (ii) lower area of steep slope corresponding to the cliff, also predominantly blue in Fig. 4a, except the northernmost area, and (iii) intermediate area in which forest vegetation grows and the movement of the treetops gives a false pattern of apparently generalized movement. Although herbaceous, shrub and forest

https://doi.org/10.5194/nhess-2021-16
Preprint. Discussion started: 19 February 2021


Natural Hazards and Earth System Sciences Discussions

vegetation, mainly eucalyptus, is profuse in this area, the field data and the comparison between the DSM carried out from the photogrammetric flights done by the Cárabo S3 aircraft in 2018 and 2019 have allowed to observe important changes occurred in some areas of the slope of the Tazones Lighthouse surroundings. Thus, the evolution of the cracks can be related to a primary planar landslide following S0 bedding and secondary movements such as flows, topples or rock fall, as has been observed in other areas of soft cliffs (Hobbs et al., 2020). Fig. 4a shows the changes in the surface of the slope and the spatial distribution of the slope instability evidence. In detail, it is possible to appreciate differences that can be attributed to the present movement of the slope, mainly in four areas: (1) the area b at the foot of the cliff, where sliding and topple processes have occurred (Fig. 4b); (2) the area c (Fig. 4c) is undergoing gradual changes since the start of monitoring, with a 100-m-long crack currently connecting the restaurant area with the lower part; (3) the westernmost part of the study area in which the presence of the sliding plane developed in November 2019 and represented in Fig. 4d, stands out; (4) the area e on the current active cliff, where evidence of sliding, rock fall and flow processes can be recognized (Fig. 4e).

The field observations allow us to deduce that the three preferential discontinuity systems facilitate the isolation of blocks that move until they fall and accumulate as blocks and debris at the foot of the cliff. As previously explained, the bedrock of the area is constituted by the Lastres Formation, an alternation of different mechanical resistance rocks, in which sandstone are mainly composed of quartz. They appear in 1-10 m packs, alternating with 5-15 m of marl and lutite layers. The presence of this diverse lithology, together with the disposition of the stratification (S0) and the presence of J1 and J2 joints offers a situation that favors the slope movement. In fact, the planar slide showed in Fig. 4d was developed following S0 in November 2019. As it has previous said, the sandstones belonging to Lastres Fm. have both quartz and carbonate cement. The actual exposition of the sandstone to the meteoric waters, through joints, faults and stratification surfaces, together with the acidity of the organic matter of the soil, cause dissolution processes of ferrous calcite cement. This process progresses relatively quickly and give rise to a variable thickness of very porous sandstone with quartz cement remains. These decalcification pores are quickly filled during rainfall periods, causing a very important increase in weight which, together with the favorable bedding slope, favors the sandstone blocks to slide. Moreover, the marls and the marly shell beds probably work as slipping levels due to their plastic (ductile) behavior during these raining periods.

In the Asturian Jurassic coast, the presence of a diverse lithology, sometimes weathered, together with the disposition of the stratification respect to the coastline enhances the development of great mass movements with hundreds of meters in length. This agree with Selby (1993), that established that cliff recession can be related to different factors such as: the presence of discontinuities (64%), the intact rock strength (20%), the rock weathering (10%) and the water erosion (6%). In addition to lithology, it is also important to consider the height of the cliff as a fundamental factor of cliffs retreat. Scars of ancient mass movements can be recognized along the Jurassic coast, reaching in many cases 120 meters in height. The higher the cliff, the more easily a break in favor of the bedrock discontinuities can occur, as has already been previously shown (Richards and Lorriman, 1987; Sunamura, 1992; Komar and Shih, 1993). These old scars, with dimensions and characteristics similar to those observed in the Tazones study area, suggest that high mass movements play a key role in the evolution of the Asturian Jurassic coast.

https://doi.org/10.5194/nhess-2021-16
Preprint. Discussion started: 19 February 2021


Natural Hazards and Earth System Sciences Discussions

To the northeastern end of the study area, in the lower part of the slope, cliffs appear, showing different instability evidence. Thus, at the base of the cliff, rockfall, sliding, topple and flow processes have occurred, leading to the accumulation of blocks, earth and debris deposits (Fig. 4b, e). The high slopes, together with the lithological and structural factors previously mentioned control this variety of processes.

Regarding the cliff retreat, field observations and photographic analysis suggest that it occurs gradually, as evidenced by the presence of cracks already in the 2001 photographs. This is in line with what has been established by previous authors, who indicate that, depending on the lithology, the evolution of the cliffs occurs on scales from 10 to 70 years (Costa et al., 2019). Until now, hillside material is slowly released in the surroundings of the Tazones Lighthouse and a sudden movement of a large volume of material towards the foot of the cliff has never been observed. This allows us to hypothesize that the evolution of the cliffs on this stretch of coast could have occurred in the same way in the recent past and may continue to function in the same way in the near future, that is, without involving large volumes of material in a single episode.

No evidence of the existence of jet mining galleries has been recognized during the field work performed in the study area and, therefore, the role that it could play in the development of the mass movement remains unknown.

3.2 Slope displacement for the period June 2018 – May 2020: quantitative measurements and relationships with rainfall

Table 2 summarizes all data recorded regarding 3D accumulated displacement of the 38 monitored markers (Fig. 1c, Fig. 5). They are organized by ranking of the obtained displacement results and classified in 9 intervals. Some of them appear without data, as previously explained in the Methodology section. Monthly measurements in Table 2 reflect in some cases small changes (1-2 cm increment or decrement) that may be attributable to the precision of the measurement method.

The analysis of the markers displacement from June, 12 2018 to May, 18 2020 has revealed that some of them have remained almost static, while others have experienced different displacement values of 3D accumulated displacement reaching even more than 15 meters (FG3). Thus, there are 10 markers, whose 3D accumulated displacement is equal to or less than 5 cm (FA2, FA4, FA6, FA10, FB3, FB5, FB6, FB7, FD5 and FE4). These 10 markers and the areas in which they were installed are considered to have remained stable during the measurement period (Fig. 5).

The remaining 28 markers have experienced 3D accumulated displacement between 6 cm (FB1 and FB4) and 15.08 cm (FG3) throughout the 2 monitoring years. Likewise, the markers displacement is uneven in time. There are some of them that have a similar behavior during all measurements (i.e. FB2, FC5) while others present a kind of acceleration in some campaigns. The highest measured displacements correspond to the C7 and C15 campaigns. In the first one (February 2019), 16 markers registered displacements above 30 cm, and 12 of them above 50 cm. In the second one (November 2019), the FG3 marker registered the largest 3D movement detected for a single campaign, moving 14.06 m in the lapse October-November 2019; also 19 of the 38 markers moved more than 30 cm in one month, reaching four of them (ARB, FF1, FG2, FG1) values equal or higher than 1 m (respectively, 1.70 m, 1.21m, 1.03 m, 1.00 m). The obtained rates, although they are measured on the slope and do not strictly correspond to the cliff retreat, are in line with those obtained by Hobbs et al. (2020) on the Holderness coast.

https://doi.org/10.5194/nhess-2021-16
Preprint. Discussion started: 19 February 2021


Natural Hazards and Earth System Sciences Discussions

The arrows in Fig. 5 show the displacement vectors together with the rank of displacement values presented in Table 2. As it can be seen, the vectors are mostly oriented to N-NNE and NE, showing the direction of the movement, which is consistent with the dip of S0 (360/15-17), described in the previous section. The evolution of the Tazones Lighthouse slope is also highly conditioned by the orientation of the coast with respect to discontinuities such as S0 and family joints, as has already been highlighted in other areas (Francioni et al., 2018). The S0 is oriented towards the coast cliff.

The temporal evolution of the displacement of one of the faster markers is presented in Fig. 6 that shows horizontal (Hz) and vertical (V) movement registered by the marker FA3. Red dots indicate the position of the marker registered in each campaign and the green/orange lines represent the inferred evolution of the movement between campaigns. The green line indicates how the movement has progressed in plant, with respect to the North; the orange one illustrates the movement with respect a horizontal plane. This marker has monthly 3D absolute displacements ranging from 1 to 38 cm, with an almost straight plan path and also a discontinuous vertical movement clearly conditioned by the S0 angle (15-17 towards the North). Thus, Fig. 6 illustrates how this marker has experienced discontinuous movement both spatially and temporally.

The distribution of the precipitation registered in the AEMET Luces-Aspo rain gauge from June 2018 to May 2020 and its relationship with the soil moisture content evolution and the displacement of six selected markers are shown in Fig. 7. Considering the variable almost monthly periodicity of the topographic control, the correlation between daily precipitation, soil moisture content and displacement cannot be addressed at a daily scale. Thus, the calculation of the precipitation between measurement campaigns (Fig. 7a) and the accumulated precipitation (Fig. 7c) has facilitated the correlation of these parameters. The periods January-February 2019 and October-November 2019 show high values of accumulated precipitation between campaigns, reaching 646 mm and 559 mm, respectively. These periods are coincident with the maxima daily rainfall values reached during the study interval: in January 22, 2019 (64.5 mm) and October 19, 2019 (82.1 mm) (Fig. 7a). Concerning the soil moisture content, this parameter shows sudden increases linked to these rainfall peaks, reaching the saturation very quickly and maintaining values above 85-90% the subsequent months (Fig. 7b). In coincidence with these periods, Fig. 7c shows two significant increases in the trend of the accumulated rainfall graph (Fig. 7c).

The comparison of the climatic series with the displacement recorded during the aforementioned periods show a good correlation between them, with a clear rise of the displacement in accordance to the rainfall and soil moisture content increases, which allows the definition of two events of acceleration of displacement (particularly in the markers FG1, FF1 or FG3). As may be seen in Fig. 7, during the periods that register the most relevant displacements, January-April 2019 and October 2019-March 2020, soil moisture content shows values above 90% most of the time.

It is worthwhile to mention the evolution of the mass movement displacement registered in the markers FC3, FD3, FG1 and FF1 after the second rainfall peak, between January and May 2020. Displacement shows a gradual reduction until April 2020. In May, the movement is almost inappreciable with respect to the previous campaign. During this period, accumulated precipitation shows a stable trend, as may be seen in the evolution of the accumulated precipitation graphic (Fig. 7c). However, a reduction in daily rainfall and an increase in the length of no-rain periods is observed. This fact, together with the increase of the evapotranspiration effect due to the seasonal transition, explain the gradual decreasing of the soil moisture content to

https://doi.org/10.5194/nhess-2021-16
Preprint. Discussion started: 19 February 2021

values under 90%. Thus, the disappearance of the conditions close to saturation may be correlated with the displacement reduction.

Table 3 shows the values of displacement measured for the most active markers during the two major events of rainfall and soil moisture content increase. In February 2019, 17 markers presented a displacement in one month that represents between 12.81 and 48.76% of the 3D accumulated displacement in the 21 control campaigns. In February 2019, 3 of these markers experienced a displacement that constitutes, respectively, 25.97% (FG2), 66.48% (ARB) and 93.25% (FG3) of the total in the two years of measurements. It is noteworthy that the FG3 marker, which is the one that has accumulated the most absolute displacement, had only moved 0.66% of the total movement until February 2019. Overall, the 3D movement of 20 markers detected in the two campaigns of February and November 2019 represents a percentage of the total 3D movement that ranges between 23.53% and 93.91%. It is also necessary to highlight that 12 of the 20 markers correspond to those that were placed in the second batch and, despite it, they accumulate significant displacements, as is the case of ARB (66.48%), FC2, CA7, FD2, FC1, FE1, FD1, FH1, FE2 and FG1 (30-40%).

The temporal distribution of the displacement previously mentioned highlight the episodic character of the mass movement activity, conditioned by the occurrence of heavy rainfall events that produce sudden rise of the soil moisture content, reaching values above 90% sustained over time during weeks or months. The use of the AWC index to represent the soil moisture content evolution have some limitations, since it has been calculated considering the behavior of a soil of a certain depth while the majority of the displaced mass is composed of materials from the bedrock. However, the sandstone of the Lastres Fm. is weathered and characterized by a relevant porosity, so in this case the AWC index could be used to estimate the saturation of its pores linked to rainfall peaks. Thus, the evolution of the displacement could be controlled by the water filling of the porosity, which implies an increase in weight of the remobilized materials, more than by the daily rainfall, since the evolution of the soil moisture content is also controlled by other factors, such as the previous soil moisture conditions or changes in the temperature. However, the infiltration of water through the cracks to the basal slide surface may also play a relevant role in the evolution of the displacement.

Although a specific study of wave dynamics has not been carried out, it is probable that the influence of precipitation and soil moisture content is more important in the stability of the cliff than the energy of the waves, as has been shown in other rocky coasts (Young et al., 2009). The accumulations of blocks are more abundant than the pebble beaches, which reflects the greater geomorphological activity due to gravity processes with respect to the littoral activity in the whole of the studied area (López-Toyos et al., in press). In this case, due to the orientation of the coast of the studied section, the storms with maximum wave energy, that always come from the northwest (Izaguirre et al., 2011), would not directly affect.

In view of the markers movement rates observed, despite that observations suggest that cliff retreat occurs gradually, the area could be dangerous for visitors who come to see and enjoy the lighthouse, the paleontological heritage or the coastal tourist trail. For this reason, the research team of this project has carried out an awareness campaign, informing the authorities who have installed warning signs both at the top, near the lighthouse, and at foot of the cliff.

https://doi.org/10.5194/nhess-2021-16
Preprint. Discussion started: 19 February 2021


Natural Hazards and Earth System Sciences Discussions

4 Conclusions

The Tazones Lighthouse slope shows a complex evolution that, from a spatial point of view, is linked to the bedrock lithology and structure. The sliding of a large part of the slope take place following the low angle bedding (S0, 360/15-17) and is manifested through different evidence such as the progressive opening of conjugated tension cracks related to two families of joints: (J1 and J2, dipping respectively 262/85 and 166/75).

The displacement take place mainly to the North-NorthEast, in accordance with the S0 dipping following marl layers. The instability is a complex mass movement with a primary planar landslide type, at least in the highest part of the slope, with secondary movements such as flows, topples or rock fall that take place in the cliffs at the bottom and the laterals of the remobilized mass.

Since the beginning of the 3D monitoring, in June 2018, until May 2020, 19 of the 38 topographic markers have moved more than 1 meter (47.4%) and 17 of the 38 markers have moved more than 2 meters, one of them (FG3) exceeding 15 m of displacement.

The comparison of displacement data with rainfall data has led to relate the evolution of the 3D movement with precipitation and soil moisture content, being able to establish a very good correlation between both. The rapid filling of the secondary porosity of Lastres Fm. sandstone by rainwater, greatly increase its weight, which favors the sliding. Thus, the greatest displacements registered in the markers have occurred after 2 periods of heavy rain in January and October-November 2019, with maximum 24 h rainfall of 64.5 mm and 82.1 mm, respectively, and values of soil moisture content above 90%. A total of 19 of the 38 markers moved more than 30 cm between October and November 2019. In February 2019, 16 markers registered displacements above 30 cm.

We conclude that the present evolution and the ancient scars that can be recognized along the coastal cliffs of the Asturian Jurassic Coast is conditioned by geological factors (bedrock lithology and structure) and climatic factors (rainfall and soil moisture), but taken into account what is happening nowadays around the Tazones Lighthouse slope, large-volume deep landslides are not expected. This research improve the understanding of the role played by landslides in coastal retreat and provides a solid knowledge base to perform predictive models of coastal retreat in future scenarios.

Code/Data availability

Currently the data is not in a repository, but if necessary it would be posted in the repository of the University of Oviedo.

Author contribution

M.J. Domínguez-Cuesta (MJDC) was responsible of field works, processing digital information by GIS and prepared the manuscript with contributions from all co-authors. P. González-Pumariega conducted the topographic markers installation and made the monthly topographical auscultation operations with the help of MJDC, C. López-Fernández (CLF), P. Valenzuela

https://doi.org/10.5194/nhess-2021-16
Preprint. Discussion started: 19 February 2021

360 (PV), J. Cuervas Mons and M. Jiménez-Sánchez (MJS). PV and M. Mora carried out the installation of a rain gauge and the precipitation and soil moisture data compilation and analysis with the help of Mónica Meléndez and Fernando Herrera; CLF and Luis Pando carried out the geomechanical characterization of the cliffs' bedrock and developed 3D models; M.A. Marigil supervised with MJDC the annually photogrammetric surveys by Remotely Piloted Aircraft and participated in photointerpretation; MJS contributed to the data analysis and integration. MJDC and MJS were the Co-Leaders of the Research
365 Project. All the coauthors contributed to the final discussion of data and final version of the paper.

Competing interests

There is no conflict of interests.

Acknowledgements

370 This research is part of the "COSINES" Project [CGL2017-83909-R], Call 2017 for RETOS Projects funded by the Spanish Economy, Industry and Competitiveness Ministry-Ministerio de Economía, Industria y Competitividad (MINECO), the Spanish Research Agency-Agencia Estatal de Investigación (AEI) and the European Regional Development Found (FEDER) and the GEOCANCOSTA research group, supported by the Asturian Regional Government (Spain) [grant number GRUPIN-
375 IDI-2018-184].

The authors thank Carlos Espadas of INGECOR GEOMÁTICA for the drone flights, José Carlos García-Ramos of MUJA for sharing us his knowledge about Lastres Fm., and the City Council and Civil Protection of the Villaviciosa municipality for the opportunity provided to analyze the cliff from a boat from the sea.

References

380 Athanasiou, P., van Dongeren, A., Giardino, A., Giardino, A., Vousdoukas, M. I., Ranasinghe, R., and Kwadijk, J.: Uncertainties in projections of sandy beach erosion due to sea level rise: an analysis at the European scale, Sci. Rep., 10, 11895, https://doi.org/10.1038/s41598-020-68576-0, 2020.

Bahamonde, J., Cossio, J., Muñoz de la Nava, P., and Cembranos, V.: Posibilidades de Azabaches en Asturias, IGME, Madrid, 1986.

385 Bird, E.: Coastal Geomorphology, an Introduction, Wiley, New York, United States of America, 2008.

https://doi.org/10.5194/nhess-2021-16
Preprint. Discussion started: 19 February 2021


Natural Hazards and Earth System Sciences Discussions

Blasco, J. J. S., Gómez-Lende, M., Sánchez-Fernández, M., and Serrano-Cañadas, E.: Monitoring retreat of coastal sandy systems using geomatics techniques: Somo Beach (Cantabrian Coast, Spain, 1875-2017), Remote Sens. 10, 1500, https://doi.org/10.3390/rs10091500, 2018.

Botey, R., and Moreno, J.: Metodología para estimar la humedad del suelo mediante un balance hídrico exponencial diario (Balance hídrico 2), AEMET, Madrid, Spain, 2012.

Boualla, O., Mehdi, K., Fadili, A., Makan, A., and Zourarah, B.: GIS-based landslide susceptibility mapping in the Safi region, West Morocco, Bull. Eng. Geol. Environ., 78, 2009–2026, https://doi.org/10.1007/s10064-017-1217-y, 2019.

Castedo, R., de la Vega-Panizo, R., Fernández-Hernández, M. and Paredes, C.: Measurement of historical cliff-top changes and estimation of future trends using GIS data between Bridlington and Hornsea – Holderness Coast (UK), Geomorphology, 230, 146–160, https://doi.org/10.1016/j.geomorph.2014.11.013, 2015.

Costa, S., Maquaire, O., Letortu, P., Thirard, G., Compain, V., Roulland, T., Medjkane, M., Davidson, R., Graff, K., Lissak, C., Delacourt, C., Duguet, T., Fauchard, C., and Antoine, R.: Sedimentary Coastal Cliffs of Normandy: Modalities and Quantification of Retreat, in: Coastal Evolution under Climate Change along the Tropical Overseas and Temperate Metropolitan France, Journal of Coastal Research, Special Issue No. 88, edited by: Castelle, B. and Chaumillon, E., Coconut Creek, Florida, United States of America, 46–60, https://doi.org/10.2112/SI88-005.1, 2019.

Domínguez-Cuesta, M.J., Valenzuela, P., Jiménez-Sánchez, M., Rodríguez-Rodríguez, L., and Ballesteros, D.: Slope instabilities in the Asturian coast (N of Iberian Peninsula): a preliminary overview, EGU General Assembly, Vienna, Austria, 8-13 April 2018, EGU2018-13525, 2018.

Domínguez-Cuesta, M.J., Valenzuela, P., Rodríguez-Rodríguez, L., Ballesteros, D., Jiménez-Sánchez, M., Piñuela, L., and García-Ramos, J.C.: Cliff coast of Asturias, in: The Spanish coastal systems, Dynamic processes, sediments and management, edited by Morales, J.A., Springer, Berlin, Heidelberg, Germany, 49-77, https://doi.org/10.1007/978-3-319-93169-23, 2018.

Domínguez-Cuesta, M.J., López-Fernández, C., González-Pumariega, P., Valenzuela, P., Marigil, M.A., Jiménez-Sánchez, M., Mora, M., Ballesteros, D., Rodríguez-Rodríguez, L., Pando, L., Meléndez, M., Flor, G., Espadas, C., Zêzere, J.L., Oliveira, S.C., Alcántara, J., and Bobrowsky, P.: Slope instability as a proxy of Cantabrian Coast retreat (N Iberia): a multidisciplinary approach, EGU General Assembly, Vienna, Austria, 7-12 April 2019, EGU2019-9729-1, 2019.

Domínguez-Cuesta, M.J., Ferrer Serrano, A., Rodríguez-Rodríguez, L., López-Fernández, C., and Jiménez-Sánchez, M.: Analysis of the Cantabrian Coast retreat around the Peñas Cape (Asturias, N Spain), Geogaceta, 68, 63-66.

Domínguez-Cuesta, M.J., González-Pumariega, P., Valenzuela, P., López-Fernández, C., Herrera, F., Mora, M., Meléndez, M., Marigil, M.A., Espadas, C., Cuervas-Mons, J., Pando, L., and Jiménez-Sánchez, M.: The fast evolution of the Tazones Lighthouse landslide (N Spain): multidisciplinary 3D monitoring between 2018 and 2019, EGU General Assembly, Online, 4-8 May, EGU2020-10175, 2020.

Emery, K.O., and Kuhn, G.G.: Sea cliffs, their processes, profiles and classification, Geol. Soc. Am. Bull., 93, 644–654, https://doi.org/10.1130/0016-7606(1982)93<644:SCTPPA>2.0.CO;2, 1982.

https://doi.org/10.5194/nhess-2021-16
Preprint. Discussion started: 19 February 2021

Epifânio, B., Zêzere, J.L., and Neves, M.: Identification of hazardous zones combining cliff retreat rates with landslide susceptibility assessment, J. Coast. Res., 65, 1681-1686, https://doi.org/10.2112/SI65-284.1, 2013.

EUROSION: Living with coastal erosion in Europe: sediment and space for sustainability: part I – major findings and policy recommendations of the EUROSION project, European Commission, Directorate General Environment, Brussels, Belgium, Open Rep., 164 pp., 2004.

Flor, G., and Flor-Blanco, G.: An introduction to the erosion and sedimentation problems in the coastal regions of Asturias and Cantabria (NW Spain) and its implications on environmental management, J. Coast. Res., 49, 58–63, http://www.jstor.org/stable/25737405, 2005.

Flor, G., Flor-Blanco, G., and Rey, J.: Dynamics and morpho-sedimentary interactions in the lower mesotidal estuary of Villaviciosa (NW Spain): A management proposal, Geologica Acta, 13, 107–121, https://doi.org/10.1344/GeologicaActa2015.13.2.3, 2015.

Flor-Blanco, G., Pando, L., Morales, J.A., and Flor, G.: Evolution of beach-dune fields systems following the construction of jetties in estuarine mouths (Cantabrian coast, NW Spain), Environ. Earth. Sci., 73, 1317–1330, https://doi.org/10.1007/s12665-014-3485-1, 2015.

Francioni, M., Coggan, J., Eyre, M., and Stead, D.: A combined field/remote sensing approach for characterizing landslide risk in coastal areas, Int. J. Appl. Earth. Obs. Geoinformation, 67, 79–95, https://doi.org/10.1016/j.jag.2017.12.016, 2018.

García Couto, M.A.: Iberian climate atlas, AEMET (España) and Instituto de Meteorología (Portugal), Madrid, Spain, 2011.

García-Ramos, J. C., and Aramburu, C.: Las sucesiones litorales y marinas del Jurásico Superior. Acantilados de Tereñes (Ribadesella) y de la playa de La Griega (Colunga), Guía de campo (excursión B), V Congreso del Jurásico de España, Colunga, Spain, 2010.

García-Ramos, J.C.: El Jurásico de la costa centro-oriental de Asturias. Un Monumento Natural de alto interés patrimonial, in: Proceedings of the VII Jornadas de Geomorfología Litoral, Geotemas, Oviedo, Spain, 17-19 July 2013, 19-29, 2013.

Gómez-Pujol, L., Pérez-Alberti, A., Blanco-Chao, R., Costa, S., Neves, M., and Del Río, L.: The rock coast of continental Europe in the Atlantic, Geol. Soc. Lond. Mem., 40, 77-88, https://doi.org/10.1144/M40.6, 2014.

Hobbs, P.R.N., Jones, L.D., Kirkham, M.P., Pennington, C.V.L., Morgan, D.J.R., and Dashwood, C.: Coastal landslide monitoring at Aldbrough, East Riding of Yorkshire, UK, Q. J. Eng. Geol. Hydrogeol., 53, 101–116, https://doi.org/10.1144/qjegh2018-210, 2020.

Izaguirre, C., Méndez, F.J., Menéndez, M., and Losada, I.J.: Global extreme wave height variability based on satellite data, Geophys. Res. Lett., 38, L10607, https://doi.org/10.1029/2011GL047302, 2011.

López, M.T.: Mapa de rocas y minerales industriales de Asturias. Escala 1:200.000, IGME, Madrid, Spain, 2012.

López-Toyos, L., Domínguez-Cuesta, M.J., and Piñuela, L.: Gravity processes and palaeontological discoveries on The Dinosaur Coast (Asturias, N Spain), Geogaceta, 69, in press.

Mateos, R.M., Azañón, J.M., Roldán, F.J., Notti, D., Pérez-Peña, V., Galve, J.P., Pérez-García, J.L., Colomo, C.M., Gómez-López, J.M., Monserrat, O., Devanthèry, N., Lamas-Fernández, F., and Fernández-Chacón, F.: The combined use of PSInSAR

https://doi.org/10.5194/nhess-2021-16
Preprint. Discussion started: 19 February 2021

and UAV photogrammetry techniques for the analysis of the kinematics of a coastal landslide affecting an urban area (SE Spain), Landslides, 14, 743–754, https://doi.org/10.1007/s10346-016-0723-5, 2017.

McGranahan, G., Balk, D., and Anderson, B.: The rising tide: assessing the risks of climate change and human settlements in low elevation coastal zones, Environ. Urban., 19, 17–37, https://doi.org/10.1177/0956247807076960, 2007.

Monte Carreño, V.: El azabache. Piedra mágica, joya, emblema jacobeo, Editorial Picu Urriellu, Gijón, Spain, 2004.

Nicholls, R.J.: Planning for the impacts of sea level rise, Oceanography, 24, 144–157, https://doi.org/10.5670/oceanog.2011.34, 2011.

Peel, M.C., Finlayson, B.L., and McMahon, T.A.: Updated world map of the Köppen-Geiger climate classification, Hydrol. Earth. Syst. Sci., 11, 1633-1644, https://doi.org/10.5194/hess-11-1633-2007, 2007.

Pérez-Alberti, A., Pires, A., Freitas, L., Rodrigues, C., and Chaminé, H.I.: Shoreline change mapping along the coast of Galicia, Spain, Marit. Eng., 166, 125–144, https://doi.org/10.1680/maen.2012.23, 2013.

Pignatelli, R., Giannini, G., Ramírez del Pozo, J., Beroiz, C., and Barón, A.: Mapa geológico de España Escala 1:50.000, IGME, Madrid, Spain, Nº 15 (14-3) Lastres, 1972.

Piñuela, L.: Huellas de dinosaurios y de otros reptiles del Jurásico Superior de Asturias. Ph.D. thesis, University of Oviedo, Spain, 326 pp. 2015.

Piñuela, L., García-Ramos, J.C., Romano, M., and Ruiz-Omeñaca, J.I.: First Record of Gregarious Behavior in Robust Medium-Sized Jurassic Ornithopods: Evidence from the Kimmeridgian Trackways of Asturias (N. Spain) and Some General Considerations on Other Medium-Large Ornithopod Tracks in the Mesozoic Record, Ichnos., 23, 298-311, https://doi.org/10.1080/10420940.2016.1178640, 2016.

Rauhut, O.W.M., Piñuela, L., Castanera, D., García-Ramos, J., and Sánchez Cela, I.: The largest European theropod dinosaurs: remains of a gigantic megalosaurid and giant theropod tracks from the Kimmeridgian of Asturias, Spain, PeerJ., 6, e4963, https://doi.org/10.7717/peerj.4963, 2018.

Richards, K.S., and Lorriman, N.R.: Basal erosion and mass movement, in: Slope stability, edited by: Anderson, M.G., and Richards, K.S., Wiley, New York, United States of America, 331-357. https://doi.org/10.1002/esp.3290140308, 1987.

Komar, P.D., and Shih, S.M.: Cliff erosion along the Oregon coast; a tectonic sea level imprint plus local controls by beach processes, J. Coast. Res., 9, 747–765, https://www.jstor.org/stable/4298127, 1993.

Selby, M.J.: Hillslope Materials and Processes, Oxford University Press, Oxford, United Kingdom, 1993.

Sunamura, T.: Geomorphology of Rocky Coasts. JohnWiley and Sons, Chichester, United Kingdom, 1992.

Trenhaile, A.S. The Geomorphology of Rock Coasts. Clarendon Press, Oxford, United Kingdom, 1987.

Trenhaile, A.S.: Climate change and its impact on rock coasts. Geol. Soc. Lond. Mem., 40, 7–17, https://doi.org/10.1144/M40.2, 2014.

Turrero, P., Domínguez-Cuesta, M.J., Jiménez-Sánchez, M., and García-Vázquez, E.: The spatial distribution of Palaeolithic human settlements and its influence on palaeoecological studies: a case from Northern Iberia. J. Archaeol. Sci., 40, 4127-4138, https://doi.org/10.1016/j.jas.2013.06.003, 2013.

https://doi.org/10.5194/nhess-2021-16
Preprint. Discussion started: 19 February 2021

Valenzuela, M., García-Ramos, J.C., and Suárez de Centi, C.: The Jurassic sedimentation in Asturias (N Spain), Trabajos de Geología, 16, 121-132, https://doi.org/10.17811/tdg.16.1986.121-133, 1986.

Valenzuela, P., Domínguez-Cuesta, M.J., Mora García, M.A., and Jiménez-Sánchez, M.: A spatio-temporal landslide inventory for the NW of Spain: BAPA database, Geomorphology, 293, 11-23, https://doi.org/10.1016/j.geomorph.2017.05.010, 2017.

Valenzuela, P., Domínguez-Cuesta, M.J., Mora García, M.A., and Jiménez-Sánchez, M.: Rainfall thresholds for the triggering of landslides considering previous soil moisture conditions (Asturias, NW Spain), Landslides, 1, 273-282, https://doi:10.1007/s10346-017-0878-8, 2018.

Valenzuela, P., Domínguez-Cuesta, M. J., López-Fernández, C., González-Pumariega, P., Jiménez-Sánchez, M., Mora García, M. A., and Marigil, M. A.: Monitoring an active mass movement in the Asturias cliff coast (North of Spain): preliminary data. EGU General Assembly, Vienna, Austria, 7-12 April 2019, EGU2019-10052, 2019.

Young, A.P., Guza, R.T., Flick, R.E., O'Reilly, W.C., and Gutierrez, R.: Rain, waves, and short-term evolution of composite seacliffs in southern California. Mar. Geol., 267, 1–7, https://doi.org/10.1016/j.margeo.2009.08.008, 2009.

Young, A.P., and Carilli, J.E.: Global distribution of coastal cliffs. Earth Surf. Process. Landf., 44, 1309-1316, https://doi.org/10.1002/esp.4574, 2018.

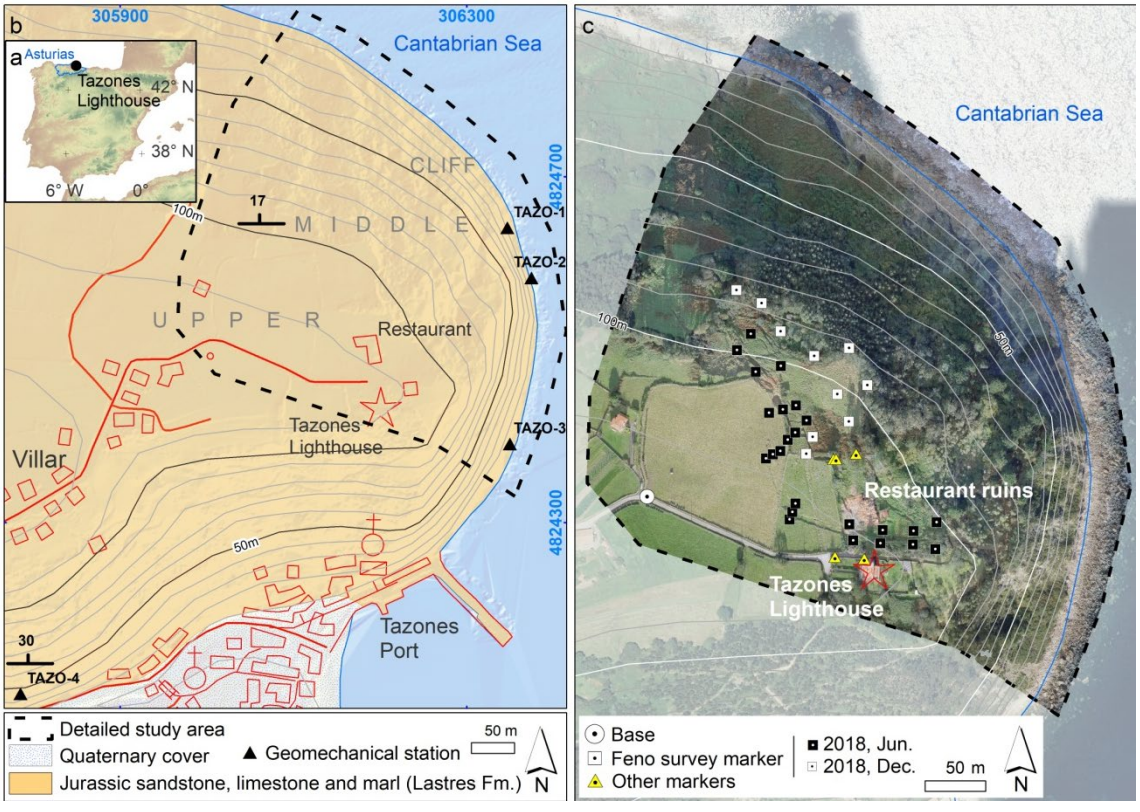

https://doi.org/10.5194/nhess-2021-16
Preprint. Discussion started: 19 February 2021

Natural Hazards and Earth System Sciences
Discussions
Open Access
EGU

Figure 1: a. Location of the study area in the Spanish Cantabrian coast. b. Parts of the slope, geological map (Pignatelli et al. 1972) and location of the geomechanical stations. LIDAR-PNOA 2012 CC-BY 4.0 scne.es. c. Position of topographic markers. OrtoPNOA 2017 CC-BY 4.0 scne.es. UTM coordinates ETRS89 Zone 30.

https://doi.org/10.5194/nhess-2021-16
Preprint. Discussion started: 19 February 2021

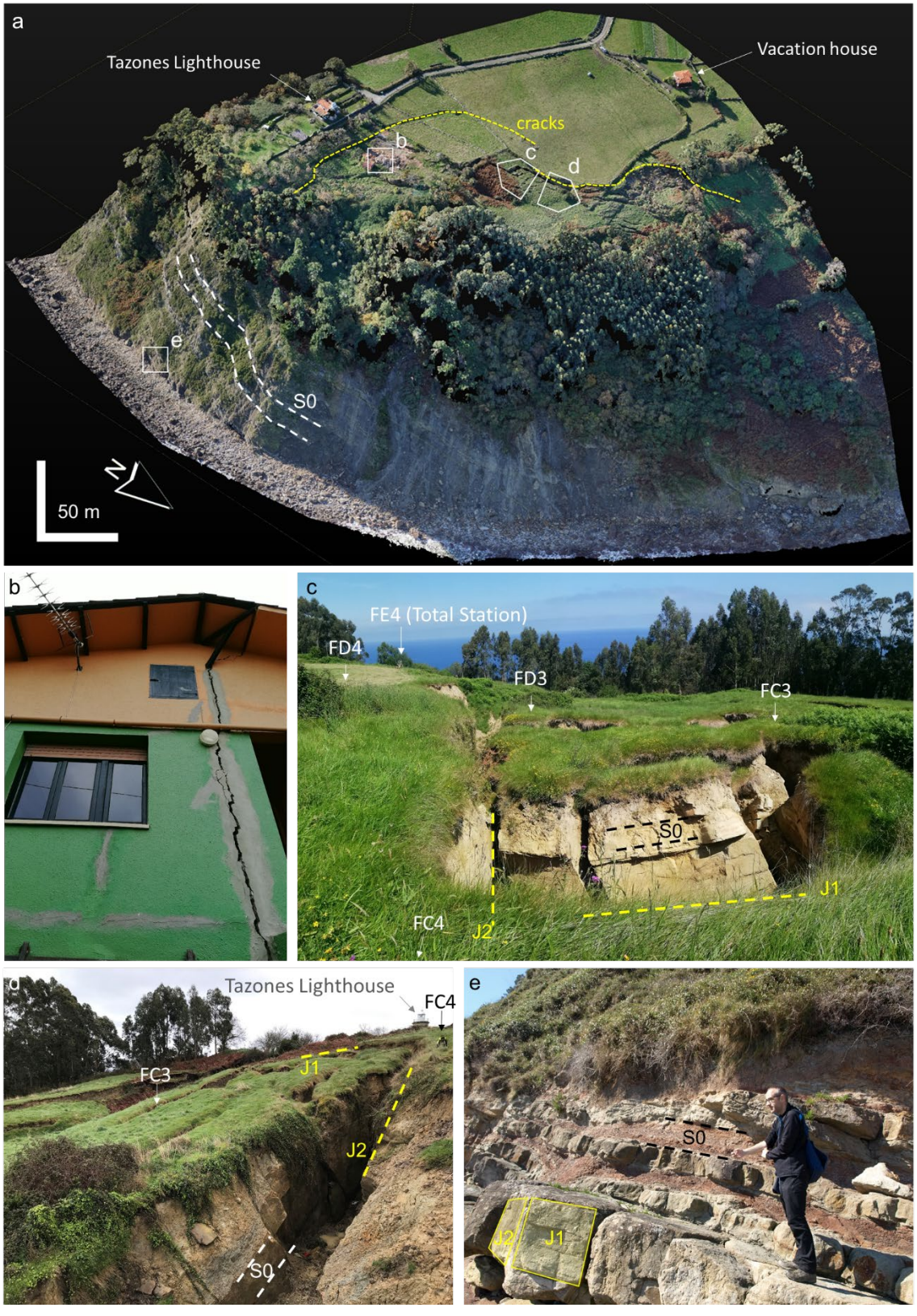

505

https://doi.org/10.5194/nhess-2021-16
Preprint. Discussion started: 19 February 2021

Natural Hazards and Earth System Sciences
Discussions

Figure 2: a. 3D view of the Tazones Ligthouse slope in the 2019 drone flight. b. Cracks in the restaurant building in 02/20/2018. The presence of cement in the wall shows the attempt to repair old cracks prior to the destructive event of February 2018. c. – d. Two views of the central part of the monitored area (FC2 - FC5 area), showing S0 and J1-J2 family joints and the position of some markers. e. Bedrock detail showing S0 and J1-J2 family joints in the bottom of the cliff.

510

https://doi.org/10.5194/nhess-2021-16
Preprint. Discussion started: 19 February 2021

Natural Hazards and Earth System Sciences
Discussions
Open Access
EGU

https://doi.org/10.5194/nhess-2021-16
Preprint. Discussion started: 19 February 2021

Natural Hazards and Earth System Sciences
Discussions
Open Access
EGU

Figure 3: Tazones Lighthouse slope evolution. a. 2001. b. 2016. c. 2018. J1 and J2 family joints are indicated. d. 2019. The yellow arrow indicates a surficial planar slide. Source: a and b, © Google Earth; c and d, drone flights carried out in this research.

https://doi.org/10.5194/nhess-2021-16
Preprint. Discussion started: 19 February 2021

Natural Hazards and Earth System Sciences
Discussions
Open Access
EGU

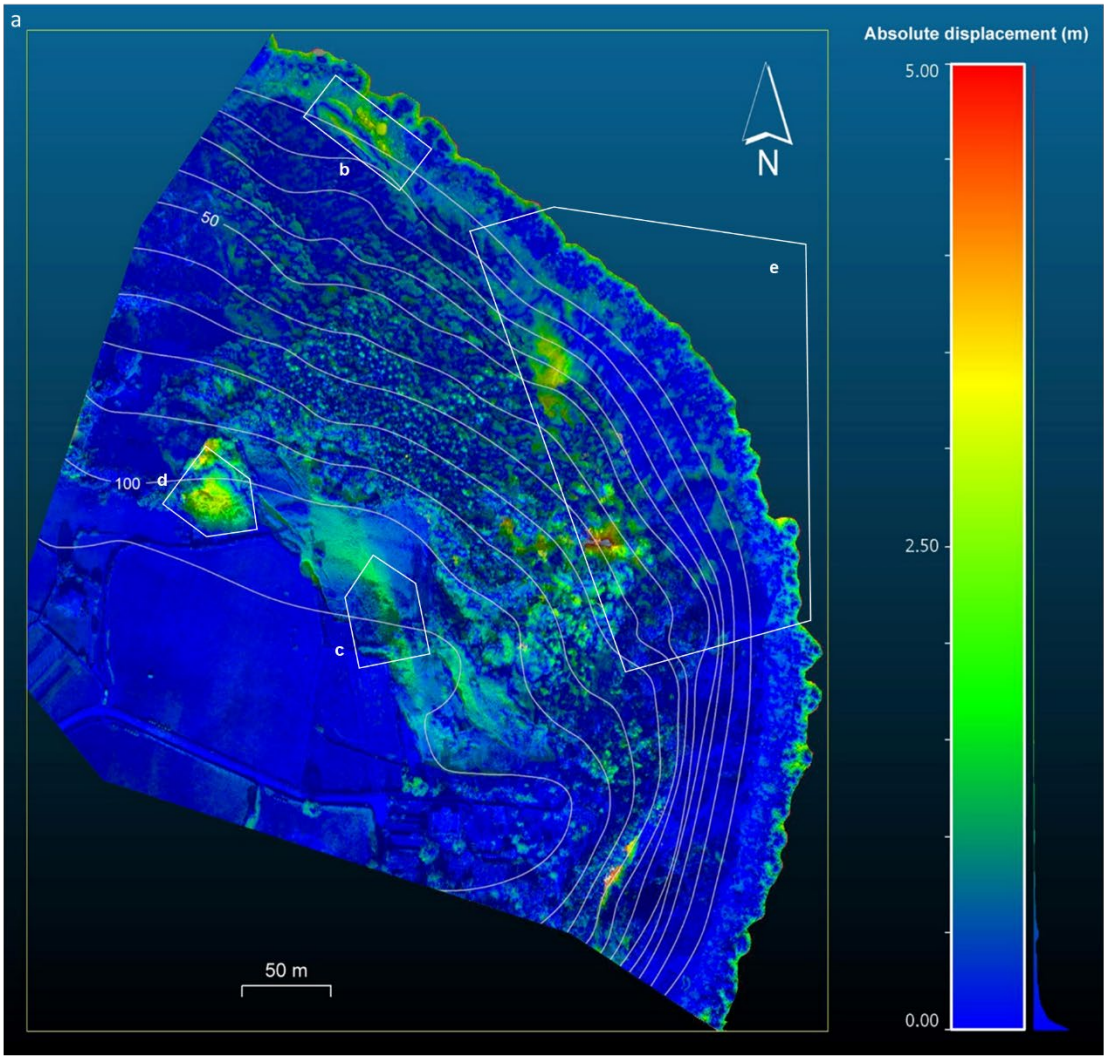

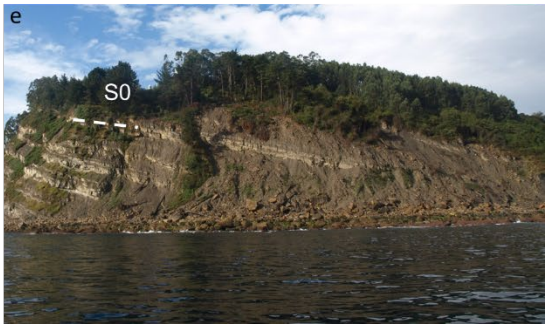

https://doi.org/10.5194/nhess-2021-16
Preprint. Discussion started: 19 February 2021

Natural Hazards and Earth System Sciences
Discussions

Figure 4: a. Surface differences between 2018 and 2019 point clouds built from Cárabo S3 aircraft drone flights. b. Detail of the foot of the cliff, showing an scarp that evolves by sliding and toppling. c. Surficial slide occurred in November 2019. d. Track that connects the Lighthouse area and the bottom of the monitored area. e. View of the cliff from the sea showing metric size block in the bottom.

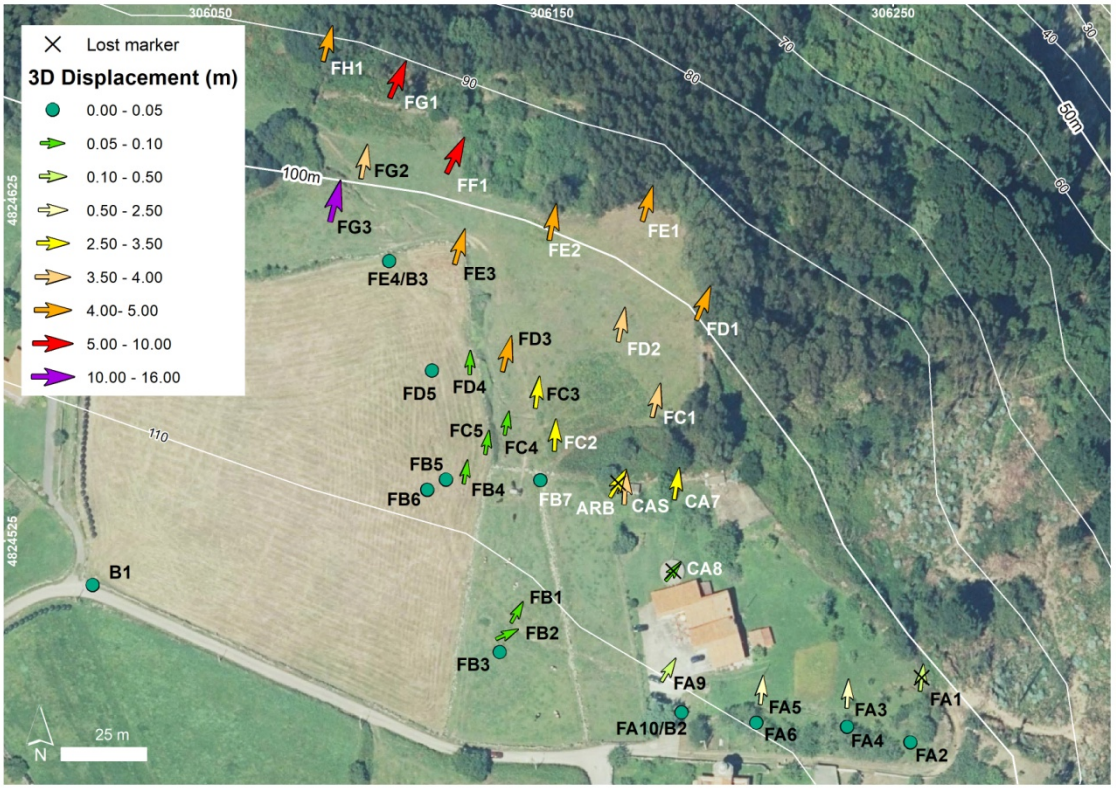

Figure 5: 3D displacement of the 38 markers monitored over the Tazones Lighthouse landslide from June 2018 to May 2020. White and black labels indicate markers of the first (June 2018) and second (December 2018) installation, respectively. OrtoPNOA 2017 CC-BY 4.0 scne.es

https://doi.org/10.5194/nhess-2021-16
Preprint. Discussion started: 19 February 2021

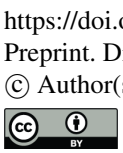

Natural Hazards and Earth System Sciences
Discussions

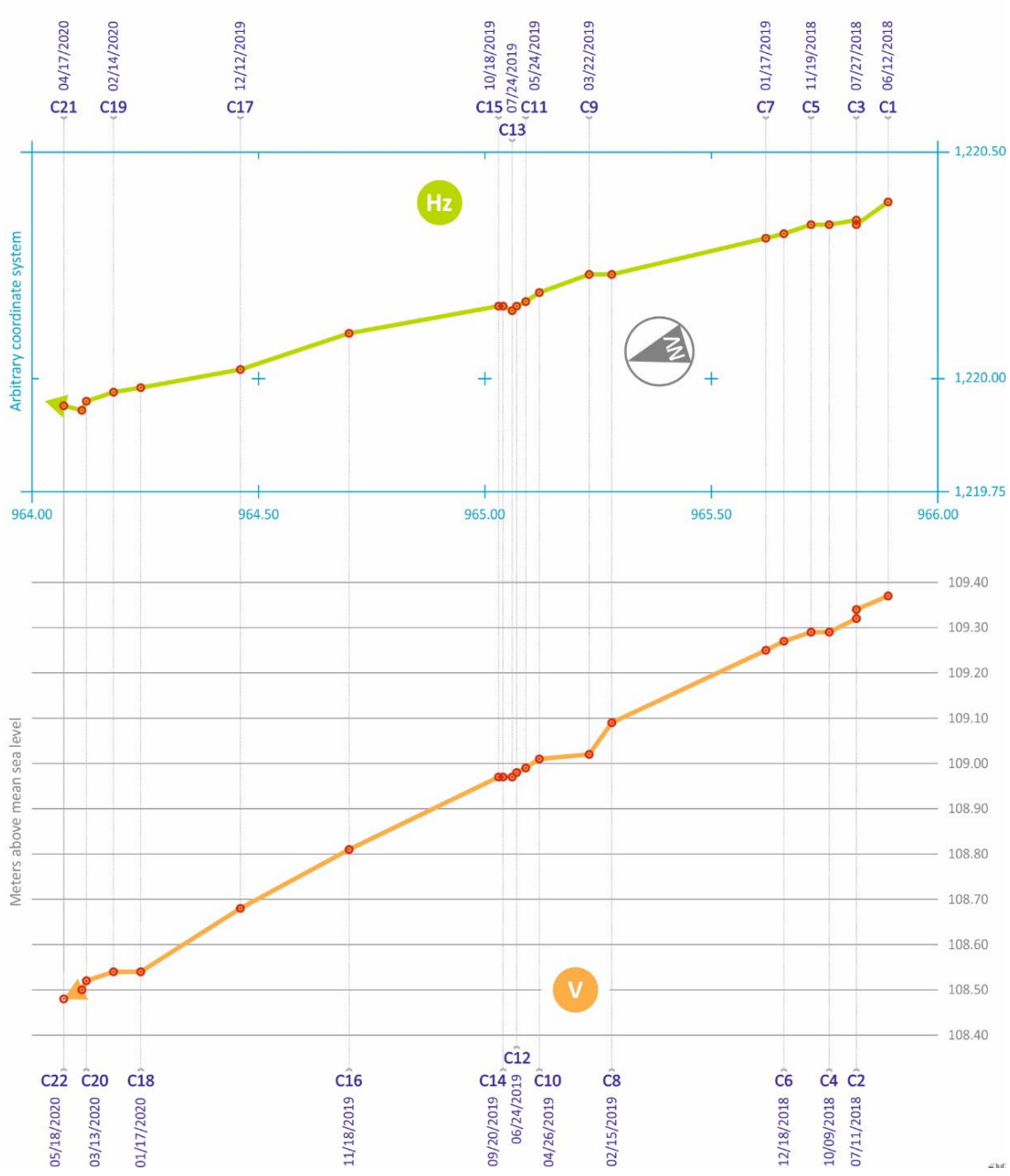

Figure 6: Time evolution of the horizontal (Hz) and vertical (V) displacement over the 22 campaigns of FA3 marker.

525

https://doi.org/10.5194/nhess-2021-16
Preprint. Discussion started: 19 February 2021

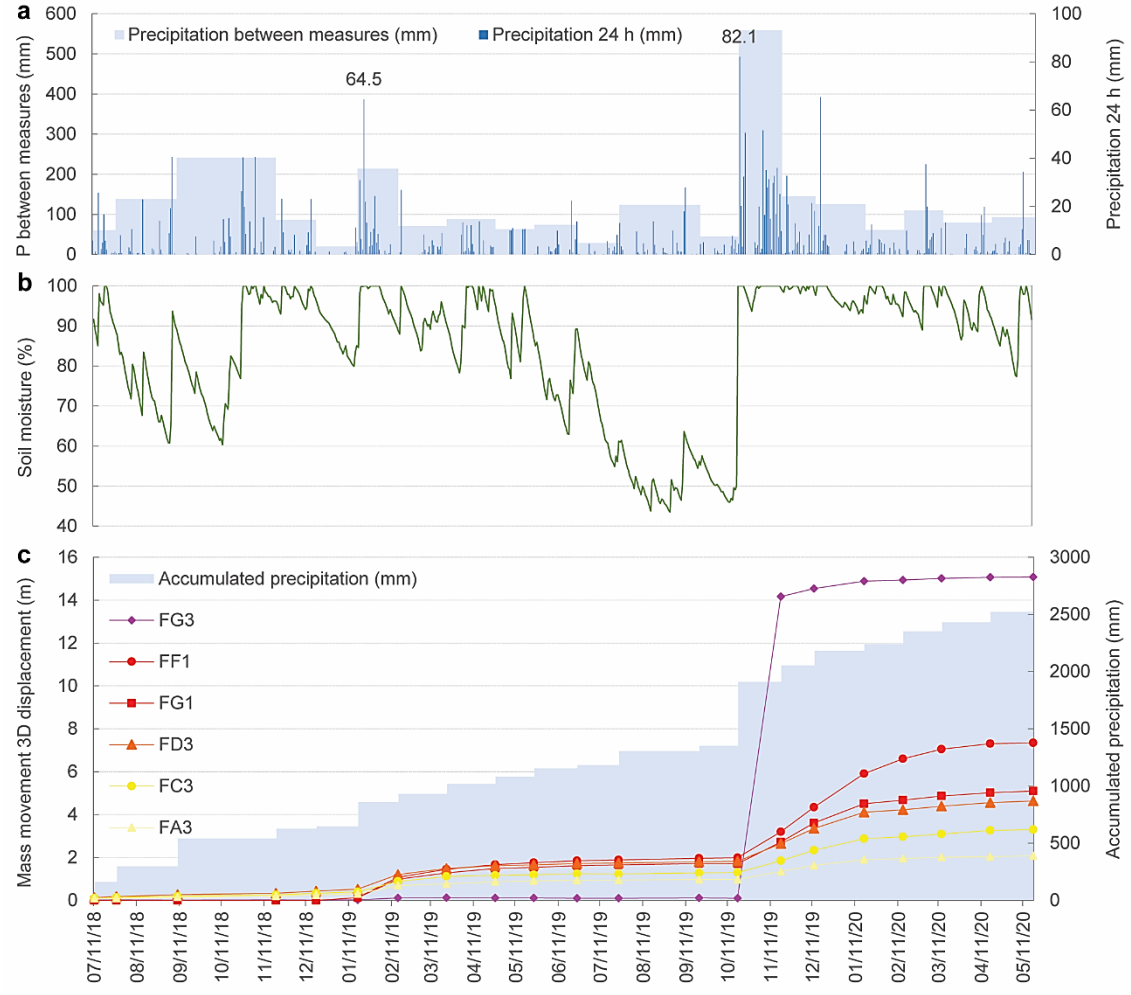

Figure 7. a. Distribution of daily rainfall vs. accumulated rainfall recorded at the Luces-Aspo rain gauge. b. Soil moisture content evolution. c. Temporal evolution of the 3D displacement of 6 selected markers vs. accummulated rainfall.

530

Table 1: Dates of the 22 monitoring campaigns carried out and days elapsed between them.

Campaign number	Date	Days between campaigns
C1	06/12/2018	Installation
C2	07/11/2018	29
C3	07/27/2018	16
C4	10/09/2018	75
C5	11/19/2018	40

https://doi.org/10.5194/nhess-2021-16
Preprint. Discussion started: 19 February 2021

Natural Hazards and Earth System Sciences
Discussions

C6	12/18/2018	28
C7	01/17/2019	31
C8	02/15/2019	29
C9	03/22/2019	35
C10	04/26/2019	35
C11	05/24/2019	28
C12	06/24/2019	31
C13	07/24/2019	30
C14	09/20/2019	58
C15	10/18/2019	28
C16	11/18/2019	31
C17	12/12/2019	24
C18	01/17/2020	36
C19	02/14/2020	28
C20	03/13/2020	28
C21	04/17/2020	35
C22	05/18/2020	31

Table 2: Accumulated displacement measured for each of the 38 markers in the 21 monitoring campaigns. Hyphen indicates campaign without measurement. Bold: markers installed in June 2018; normal letters: December 2019; italics: lost markers. Gray color indicates the greatest displacements measured between campaigns.

https://doi.org/10.5194/nhess-2021-16
Preprint. Discussion started: 19 February 2021

Natural Hazards and Earth System Sciences
Discussions

	3D acummulated displacement (m)																					
Marker	07/11/2018	07/27/2018	10/09/2018	11/19/2018	12/18/2018	01/17/2019	02/15/2019	03/22/2019	04/26/2019	05/24/2019	06/24/2019	07/24/2019	09/20/2019	10/18/2019	11/18/2019	12/12/2019	01/17/2020	02/14/2020	03/13/2020	04/17/2020	05/18/2020	3D Total displacement rank (m)
FA4	0.02	0.02	0.02	0.01	0.02	0.02	0.03	0.02	0.02	0.02	0.02	0.01	0.01	0.02	0.02	0.01	0.01	0.01	0.01	0.02	0.02	0.0 - 0.05
FB3	0.00	0.02	0.02	0.01	0.02	0.01	0.02	—	0.02	0.02	0.02	0.01	0.02	0.01	0.02	0.01	0.01	0.01	0.02	0.02	0.02	
FA2	0.03	0.01	0.03	0.02	0.03	0.03	0.02	0.02	0.02	0.03	0.04	0.02	0.01	0.03	0.03	0.01	0.01	0.02	0.02	0.02	0.02	
FE4	0.02	0.03	0.01	0.02	0.01	0.03	0.03	0.02	0.03	0.02	0.02	0.01	0.01	0.02	0.03	0.03	0.02	0.02	0.02	0.02	0.02	
FB7	—	—	—	—	—	0.01	0.02	—	0.03	0.03	0.02	0.01	0.01	0.02	0.02	0.01	0.03	0.03	0.03	0.03	0.02	
FA6	0.02	0.01	0.02	0.01	0.01	0.02	0.01	—	0.01	0.02	0.02	0.01	0.02	0.04	0.01	0.01	0.01	0.01	0.01	0.03	0.02	
FA10	0.01	0.00	0.01	0.02	0.02	0.02	0.01	—	0.01	0.01	0.01	0.01	0.03	0.03	0.03	0.02	0.02	0.03	0.03	0.02	0.03	
FB6	0.01	0.02	0.01	0.02	0.02	0.02	0.02	0.02	0.03	0.03	0.01	0.02	0.03	0.02	0.01	0.01	0.02	0.02	0.01	0.02	0.03	
FB5	0.01	0.02	0.02	0.03	0.03	0.04	0.04	—	0.04	—	—	0.03	0.04	0.03	0.03	0.04	0.04	0.04	0.04	0.04	0.04	
FD5	0.02	0.02	0.01	0.01	0.02	0.01	0.02	—	0.02	0.02	0.01	0.05	0.04	0.05	0.04	0.02	0.04	0.03	0.04	0.04	0.05	
FB1	0.02	0.04	0.04	0.04	0.04	0.04	0.06	—	0.05	0.06	0.06	0.05	0.05	0.06	0.06	0.05	0.06	0.06	0.06	0.07	0.06	0.05 - 0.10
FB4	0.02	0.05	0.04	0.04	0.05	0.06	0.07	—	0.07	0.08	0.07	0.05	0.06	0.06	0.06	0.06	0.07	0.07	0.07	0.07	0.06	
CA8	—	—	—	—	—	*0.06*	—	—	—	—	—	—	—	—	—	—	—	—	—	—	—	
FC5	0.01	0.04	0.04	0.05	0.05	0.05	0.07	0.08	0.07	0.08	0.06	0.06	0.07	0.07	0.07	0.06	0.07	0.07	0.07	0.08	0.07	
FC4	0.01	0.05	0.04	0.04	0.07	0.07	0.09	0.09	0.10	0.08	0.08	0.06	0.08	0.06	0.08	0.07	0.08	0.07	0.08	0.09	0.07	
FD4	0.03	0.04	0.04	0.04	0.04	0.06	0.07	—	0.08	0.07	0.07	0.05	0.07	0.08	0.07	0.06	0.08	0.08	0.07	0.07	0.09	
FB2	0.02	0.03	0.04	0.05	0.05	0.07	0.07	0.09	0.09	0.08	0.08	0.08	0.09	0.08	0.08	0.08	0.09	0.09	0.09	0.09	0.09	
FA9	0.02	0.03	0.04	0.05	0.06	0.07	0.13	—	0.14	0.13	0.14	0.12	0.13	0.13	0.13	0.12	0.12	0.12	0.13	0.12	0.12	0.10 - 0.50
FA1	*0.08*	*0.07*	*0.13*	*0.18*	*0.25*	*0.29*	—	—	—	—	—	—	—	—	—	—	—	—	—	—	—	
FA5	0.08	0.09	0.15	0.19	0.22	0.28	0.61	0.73	0.77	0.79	0.82	0.83	0.85	0.86	1.16	1.39	1.60	1.61	1.66	1.67	1.71	0.50 - 2.50
FA3	0.09	0.09	0.16	0.20	0.26	0.31	0.69	0.77	0.87	0.91	0.93	0.95	0.98	0.97	1.35	1.63	1.89	1.94	2.01	2.04	2.07	
FC2	—	—	—	—	—	0.06	0.51	0.66	0.76	0.78	0.82	0.82	0.86	0.87	1.37	1.74	2.15	2.21	2.30	2.48	2.52	2.50 - 3.50
ARB	—	—	—	—	—	—	—	*0.52*	*0.49*	*0.58*	*0.66*	*0.70*	*0.79*	*0.86*	*2.56*	—	—	—	—	—	—	
FC3	0.10	0.14	0.19	0.25	0.32	0.40	0.88	1.12	1.16	1.19	1.24	1.23	1.28	1.29	1.85	2.34	2.88	2.97	3.10	3.26	3.30	
CA7	—	—	—	—	—	0.09	0.68	0.95	1.02	1.07	1.11	1.15	1.19	1.20	1.89	2.47	3.05	3.17	3.29	3.42	3.46	
FD2	—	—	—	—	—	0.11	0.75	1.04	1.11	1.16	1.21	1.22	1.28	1.29	2.01	2.62	3.21	3.31	3.44	3.56	3.63	3.50 - 4.0
FC1	—	—	—	—	—	0.11	0.76	1.02	1.12	1.17	1.20	1.22	1.28	1.30	2.03	2.64	3.24	3.35	3.48	3.61	3.70	
CAS	—	—	—	—	—	—	—	0.35	0.43	0.53	0.59	0.63	0.69	0.73	1.63	2.46	3.29	3.45	3.65	3.81	3.83	
FG2	0.13	0.16	0.22	0.31	0.37	0.46	1.08	1.26	1.38	1.41	1.44	1.45	1.50	1.51	2.53	3.11	3.65	3.75	3.86	3.93	3.97	
FE1	—	—	—	—	—	0.11	0.82	1.06	1.20	1.26	1.29	1.32	1.40	1.41	2.19	2.86	3.56	3.67	3.82	3.97	4.03	4.0 - 5.0
FD1	—	—	—	—	—	0.11	0.80	1.09	1.21	1.26	1.33	1.32	1.40	1.42	2.20	2.90	3.57	3.69	3.83	3.98	4.05	
FH1	—	—	—	—	—	0.10	0.77	0.99	1.13	1.19	1.23	1.25	1.30	1.31	2.18	2.86	3.60	3.73	3.88	3.99	4.06	
FE2	—	—	—	—	—	0.10	0.81	1.08	1.22	1.27	1.33	1.35	1.41	1.43	2.23	2.92	3.62	3.75	3.90	4.05	4.12	
FE3	0.11	0.16	0.25	0.34	—	0.52	1.23	1.48	1.63	1.69	1.74	1.77	1.83	1.84	2.64	3.32	4.01	4.12	4.28	4.41	4.47	
FD3	0.13	0.18	0.26	0.33	0.44	0.53	1.21	1.49	1.61	1.66	1.72	1.74	1.80	1.82	2.64	3.35	4.10	4.23	4.40	4.56	4.63	
FG1	—	—	—	—	—	0.13	0.98	1.29	1.48	1.54	1.61	1.65	1.72	1.71	2.72	3.61	4.50	4.67	4.87	5.03	5.10	5.0 - 10.0
FF1	—	—	—	—	—	0.13	1.07	1.45	1.67	1.76	1.85	1.88	1.96	1.99	3.20	4.34	5.91	6.60	7.04	7.30	7.34	
FG3	0.01	0.03	0.01	0.02	0.01	0.02	0.11	0.13	0.11	0.12	0.10	0.10	0.12	0.10	14.17	14.54	14.89	14.93	15.01	15.06	15.08	10.0 - 16.0

Table 3: Displacement measured for the most active 20 markers in the January-February 2019 (C6-C7) and October-November 2019 (C14-C15) monitoring campaigns. Bold: markers installed in June 2018; normal letters: December 2019; italics: lost markers.

https://doi.org/10.5194/nhess-2021-16
Preprint. Discussion started: 19 February 2021

Natural Hazards and Earth System Sciences
Discussions
Open Access
EGU

	Feb - Jan 2019 3D displacement				Nov - Oct 2019 3D displacement				Feb + Nov 2019		Total 3D displacement rank (m)
	m				m				m	%	
Marker	01/17/2019	02/15/2019	Feb - Jan 2019	%	10/18/2019	11/18/2019	Oct - Nov 2019	%	3D displacement	3D displacement	
FA9	0.07	0.13	0.06	48.76	0.13	0.13	0.00	0.00	0.12	48.76	0.10 - 0.50
FA5	0.28	0.61	0.33	19.31	0.86	1.16	0.30	17.55	1.71	36.86	0.50 - 2.50
FA3	0.31	0.69	0.38	18.33	0.97	1.35	0.38	18.33	2.07	36.66	
FC2	0.06	0.51	0.45	17.87	0.87	1.37	0.50	19.85	2.52	37.72	2.50 - 3.50
ARB	—	—	—	*0.00*	*0.86*	*2.56*	*1.70*	*66.48*	*1.00*	*66.48*	
FC3	0.40	0.88	0.49	14.84	1.29	1.85	0.56	16.96	3.30	31.79	
CA7	0.09	0.68	0.59	17.03	1.20	1.89	0.69	19.92	3.46	36.95	
FD2	0.11	0.75	0.64	17.62	1.29	2.01	0.72	19.82	3.63	37.44	3.50 - 4.0
FC1	0.11	0.76	0.66	17.84	1.30	2.03	0.73	19.73	3.70	37.57	
CAS	—	—	—	0.00	0.73	1.63	0.90	23.53	3.83	23.53	
FG2	0.46	1.08	0.61	15.38	1.51	2.53	1.03	25.97	3.97	41.35	
FE1	0.11	0.82	0.71	17.60	1.41	2.19	0.78	19.33	4.03	36.93	4.0 - 5.0
FD1	0.11	0.80	0.70	17.29	1.42	2.20	0.78	19.26	4.05	36.55	
FH1	0.10	0.77	0.67	16.50	1.31	2.18	0.87	21.42	4.06	37.92	
FE2	0.10	0.81	0.71	17.24	1.43	2.23	0.80	19.43	4.12	36.67	
FE3	0.52	1.23	0.71	15.87	1.84	2.64	0.80	17.88	4.47	33.74	
FD3	0.53	1.21	0.68	14.69	1.82	2.64	0.82	17.72	4.63	32.41	
FG1	0.13	0.98	0.85	16.67	1.71	2.72	1.00	19.61	5.10	36.28	5.0 - 10.0
FF1	0.13	1.07	0.94	12.81	1.99	3.20	1.21	16.48	7.34	29.29	
FG3	0.02	0.11	0.10	0.66	0.10	14.17	14.06	93.25	15.08	93.91	10.0 - 16.0